

# Distinct roles for ROCK1 and ROCK2 in the regulation of cell detachment

Jianjian Shi<sup>1,4</sup>, Xiangbing Wu<sup>1,4</sup>, Michelle Surma<sup>1</sup>, Sasidhar Vemula<sup>2</sup>, Lumin Zhang<sup>1</sup>, Yu Yang<sup>1</sup>, Reuben Kapur<sup>2</sup> and Lei Wei<sup>\*1,3</sup>

This study, using mouse embryonic fibroblast (MEF) cells derived from *ROCK1*<sup>-/-</sup> and *ROCK2*<sup>-/-</sup> mice, is designed to dissect roles for ROCK1 and ROCK2 in regulating actin cytoskeleton reorganization induced by doxorubicin, a chemotherapeutic drug. *ROCK1*<sup>-/-</sup> MEFs exhibited improved actin cytoskeleton stability characterized by attenuated periphery actomyosin ring formation and preserved central stress fibers, associated with decreased myosin light chain 2 (MLC2) phosphorylation but preserved cofilin phosphorylation. These effects resulted in a significant reduction in cell shrinkage, detachment, and predetachment apoptosis. In contrast, *ROCK2*<sup>-/-</sup> MEFs showed increased periphery membrane folding and impaired cell adhesion, associated with reduced phosphorylation of both MLC2 and cofilin. Treatment with inhibitor of myosin (blebbistatin), inhibitor of actin polymerization (cytochalasin D), and ROCK pan-inhibitor (Y27632) confirmed the contributions of actomyosin contraction and stress fiber instability to stress-induced actin cytoskeleton reorganization. These results support a novel concept that ROCK1 is involved in destabilizing actin cytoskeleton through regulating MLC2 phosphorylation and peripheral actomyosin contraction, whereas ROCK2 is required for stabilizing actin cytoskeleton through regulating cofilin phosphorylation. Consequently, ROCK1 and ROCK2 can be functional different in regulating stress-induced stress fiber disassembly and cell detachment.

*Cell Death and Disease* (2013) 4, e483; doi:10.1038/cddis.2013.10; published online 7 February 2013

**Subject Category:** Experimental medicine

Rho-kinase (ROCK) is one of the best-characterized effectors of small GTPase RhoA and belongs to the AGC (protein kinase A/protein kinase G/protein kinase C) family of serine/threonine kinases.<sup>1–4</sup> As a major downstream effector of RhoA, ROCK promotes actin–myosin-mediated contractile force generation by phosphorylating a variety of downstream target proteins. The major downstream substrates of ROCK include the myosin binding subunit of myosin light chain (MLC) phosphatase 1 (MYPT1),<sup>5,6</sup> myosin light chain 2 (MLC2),<sup>5</sup> LIM kinases,<sup>7,8</sup> thereby modulating actin cytoskeleton organization, stress fiber formation and smooth muscle cell contraction. ROCK can increase MLC2 phosphorylation through direct effect on MLC2 or indirectly by inactivating MLC phosphatase, resulting in stimulation of actomyosin contractility.<sup>5,6</sup> ROCK stabilizes actin filaments through LIM kinases (LIMK) activation, resulting in cofilin phosphorylation and thereby inhibiting its actin depolymerization activity.<sup>7,8</sup> Both ROCK/MYPT1/MLC2 and ROCK/LIMK/cofilin pathways are heavily involved in stress fiber assembly and cell adhesion. However, the roles of ROCK in the regulation of stress fiber disassembly and cell detachment are less well understood.

The ROCK family contains two members, ROCK1 and ROCK2; they share 65% overall identity and 92% identity in

the kinase domain.<sup>1–4</sup> Both kinases contain a catalytic kinase domain at the N-terminus, followed by a central coiled-coil domain, including a Rho-binding domain and a C-terminal pleckstrin-homology (PH) domain, with an internal cysteine-rich domain. Owing to the high degree of sequence homology, ROCK1 and ROCK2 are believed to share more than 30 immediate downstream substrates, including MYPT1, MLC, and LIMK (reviewed in refs 9–16). However, most of the studies have been performed with non-isoform-selective pharmacological inhibitors. Two commonly used ROCK inhibitors, Y27632<sup>17</sup> and fasudil,<sup>18</sup> target the ATP-dependent kinase domain, therefore inhibit ROCK1 and ROCK2 with equal potency, and also have non-selective effects.<sup>17,19,20</sup>

Regardless of the fact that the two ROCK isoforms are very similar and are possibly somewhat redundant, a growing body of evidence supports that they also have unique functions (reviewed in Surma *et al.*<sup>15</sup> and Shi *et al.*<sup>21</sup>). Using mouse embryonic fibroblast (MEF) cells derived from *ROCK1* knockout mice,<sup>22</sup> the current study reveals a novel role for ROCK1 in mediating actin cytoskeleton remodeling in response to cytotoxic stress induced by doxorubicin, a chemotherapeutic drug.<sup>23,24</sup> Doxorubicin is well known to intercalate within the

<sup>1</sup>Riley Heart Research Center, Herman B Wells Center for Pediatric Research, Department of Pediatrics, Indiana University School of Medicine, Indianapolis, IN, USA;

<sup>2</sup>Herman B Wells Center for Pediatric Research, Department of Pediatrics, Indiana University School of Medicine, Indianapolis, IN, USA and <sup>3</sup>Department of Cellular and Integrative Physiology, Indiana University, School of Medicine, Indianapolis, IN, USA

\*Corresponding author: L Wei, Riley Heart Research Center, Herman B Wells Center for Pediatric Research, Indiana University School of Medicine, 1044 West Walnut Street, R4-370, Indianapolis, IN 46202-5225, USA. Tel: + 317 274 7894; Fax: + 317 278 9298; E-mail: lewei@iupui.edu

<sup>4</sup>These authors contributed equally to this work.

**Keywords:** Rho-kinase; actin cytoskeleton remodeling; detachment; apoptosis; isoform function

**Abbreviations:** 7-AAD, 7-amino-actinomycin D; DAPI, diamidino-2-phenylindole; DMEM, Dulbecco's modified Eagle's medium; FBS, fetal bovine serum; F-actin, filamentous actin; LIMK, LIM kinases; MEF, mouse embryonic fibroblast; MLC2, myosin light chain 2; MYPT1, myosin light chain phosphatase 1; MTT, methylthiazole tetrazolium; PBS, phosphate-buffered saline; PH, pleckstrin-homology; ROCK, Rho-kinase; siRNA, small interfering ribonucleic acid; WT, wild-type

Received 27.09.12; revised 24.12.12; accepted 3.01.13; Edited by G Ciliberto

DNA, inhibit DNA topoisomerase II, and generate free radicals.<sup>25,26</sup> At the same time, doxorubicin also increases actin cytoskeleton instability via inhibition of actin polymerization.<sup>27,28</sup> We observed that ROCK1 deficiency in MEF cells inhibited actin cytoskeleton reorganization by attenuating periphery actomyosin ring formation and preserving central stress fibers, therefore resulting in decreased cell detachment and predetachment apoptosis. These protective features are unique to ROCK1 deficiency as ROCK2-deficient cells exhibited increased periphery membrane folding and altered cell adhesion. Moreover, ROCK inhibitors abolished the protective effects of ROCK1 deficiency by disrupting stress fibers. Although MLC2 phosphorylation was reduced to a similar extent in *ROCK1*<sup>-/-</sup> and *ROCK2*<sup>-/-</sup> MEFs, the profile of cofilin phosphorylation was clearly different, which likely contributes to their differential effects on actin cytoskeleton remodeling. Our results reveal that ROCK1 and ROCK2 are functionally different in regulating stress-induced actin cytoskeleton reorganization and cell detachment.

## Results

**ROCK1 deficiency, but not ROCK2 deficiency or ROCK inhibitor treatment, improves cell viability in response to doxorubicin treatment.** *ROCK1*<sup>-/-</sup> and *ROCK2*<sup>-/-</sup> MEFs in FVB background (Figure 1a) were prepared from E13.5 homozygous *ROCK1*<sup>22</sup> and *ROCK2* knockout

embryos (derived from interbreeding of *ROCK2* heterozygous mice in FVB background, Supplementary Figure 1), respectively. At baseline growth condition, both *ROCK1*<sup>-/-</sup> and *ROCK2*<sup>-/-</sup> MEFs exhibited similar proliferation rates as wild-type (WT) MEFs (Supplementary Figure 2). To test the effects of ROCK isoform deletion responding to doxorubicin treatment, we first assessed cell viability by methylthiazole tetrazolium (MTT) assay. WT cells exhibited a dose-dependent reduction of cell viability (Figure 1b). Importantly, *ROCK1*<sup>-/-</sup> cells exhibited a significant improvement in cell viability compared with WT cells (Figure 1b). Upon doxorubicin treatment at 3  $\mu$ M for 16 h, which was the condition used for most of the following experiments, cell viability in WT cells was reduced by 50–60%, but only by 10–20% in *ROCK1*<sup>-/-</sup> cells.

A similar experiment was performed with *ROCK2*<sup>-/-</sup> MEFs (Figure 1c). Different from *ROCK1*<sup>-/-</sup> cells, *ROCK2*<sup>-/-</sup> cells exhibited a trend of reduction of cell viability compared with WT cells after doxorubicin treatment, but the difference was not statistically significant. Moreover, cotreating WT cells with Y27632 significantly reduced cell viability compared with doxorubicin treatment alone, indicating that inhibition of both ROCK1 and ROCK2 enhances doxorubicin-induced cytotoxicity (Figure 1d). In the absence of doxorubicin, Y27632 ( $K_i=0.14 \mu$ M for ROCK) had no significant effect on cell viability at 5–10  $\mu$ M (Figure 1d). Similar results were observed with H1152 at 0.5 and 1  $\mu$ M, another chemical ROCK inhibitor ( $K_i=1.6$  nM for ROCK).

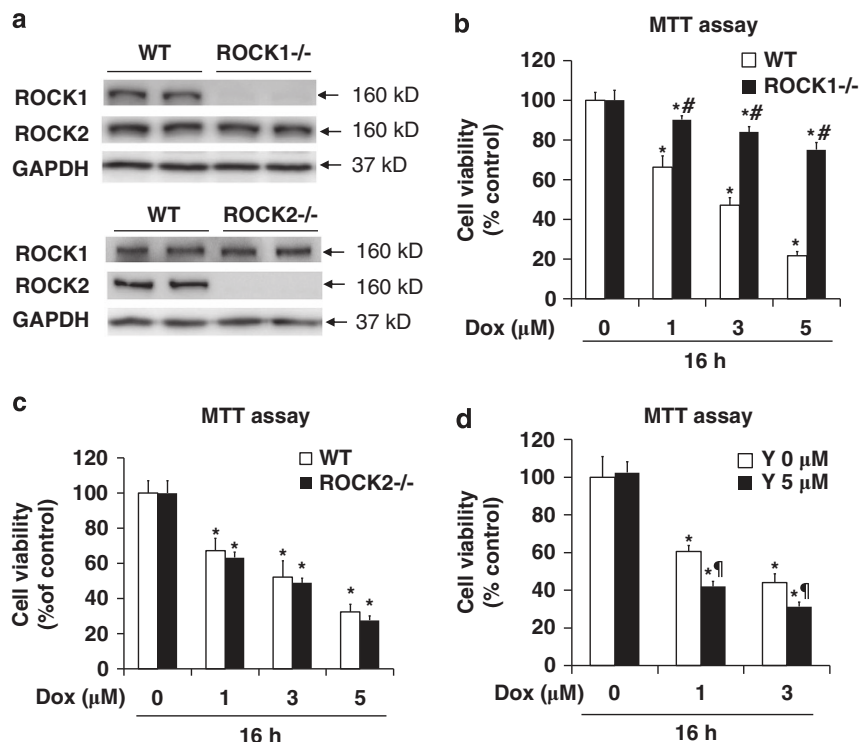


**Figure 1** ROCK1 deletion, but not ROCK2 deletion or ROCK pan-inhibition, increases cell viability in response to doxorubicin. (a) Representative image of western blot of ROCK1 and ROCK2 performed with cell lysates from WT, *ROCK1*<sup>-/-</sup>, and *ROCK2*<sup>-/-</sup> MEFs. GAPDH was used to confirm equal loading. (b and c) MTT assay performed with WT and *ROCK1*<sup>-/-</sup> MEFs or with WT and *ROCK2*<sup>-/-</sup> MEFs treated for 16 h with increasing dosages of doxorubicin as indicated. (d) MTT assay performed with WT MEFs treated for 16 h with increasing dosages of doxorubicin with or without 5  $\mu$ M Y27632. Cell viability was expressed as percentage of control cells without treatment. \* $P < 0.05$  versus control of the same genotype. # $P < 0.05$  versus WT under the same treatment condition. † $P < 0.05$  versus WT under doxorubicin only condition

**ROCK1 deficiency inhibits cell detachment in response to doxorubicin treatment.**

To determine the cellular mechanisms underlying the improved cell viability by ROCK1 deletion, we first noticed a significant increase in cell detachment of WT cells upon doxorubicin treatment, but it was delayed in *ROCK1*<sup>-/-</sup> cells (Figure 2). Bright field photography and cell counting showed a time-dependent increase in cell detachment upon doxorubicin treatment of the WT cells, while a significant reduction was observed in *ROCK1*<sup>-/-</sup> cells (Figures 2a–c). In addition, ROCK1 deficiency also reduced cell detachment at all tested dosages of doxorubicin (Figures 2d and e). The inhibiting level of cell detachment (e.g., the ratio of floating cells was 50–60% in WT cells versus 10–20% in *ROCK1*<sup>-/-</sup> cells after 3 μM doxorubicin treatment for 16 h) correlated with the improved cell viability observed in *ROCK1*<sup>-/-</sup> cells

(Figure 1b), supporting that reduced cell detachment crucially contributes to the improved cell viability of ROCK1-deficient cells from doxorubicin treatment.

**ROCK1 deficiency reduces formation of cortical contractile rings, preserves central stress fibers, and reduces cell shape changes.**

To dissect molecular mechanisms underlying the inhibitory effects of ROCK1 deletion on doxorubicin-induced detachment, we examined actin cytoskeleton remodeling. The alteration of the actin cytoskeleton is mainly driven by actin polymerization/depolymerization activities and the force exerted by myosin on actin filaments ('actomyosin contraction'). The stress fibers containing filamentous actin (F-actin) and phosphorylated MLC2 can be broadly divided into two morphological types: thick and dense stress fibers, which

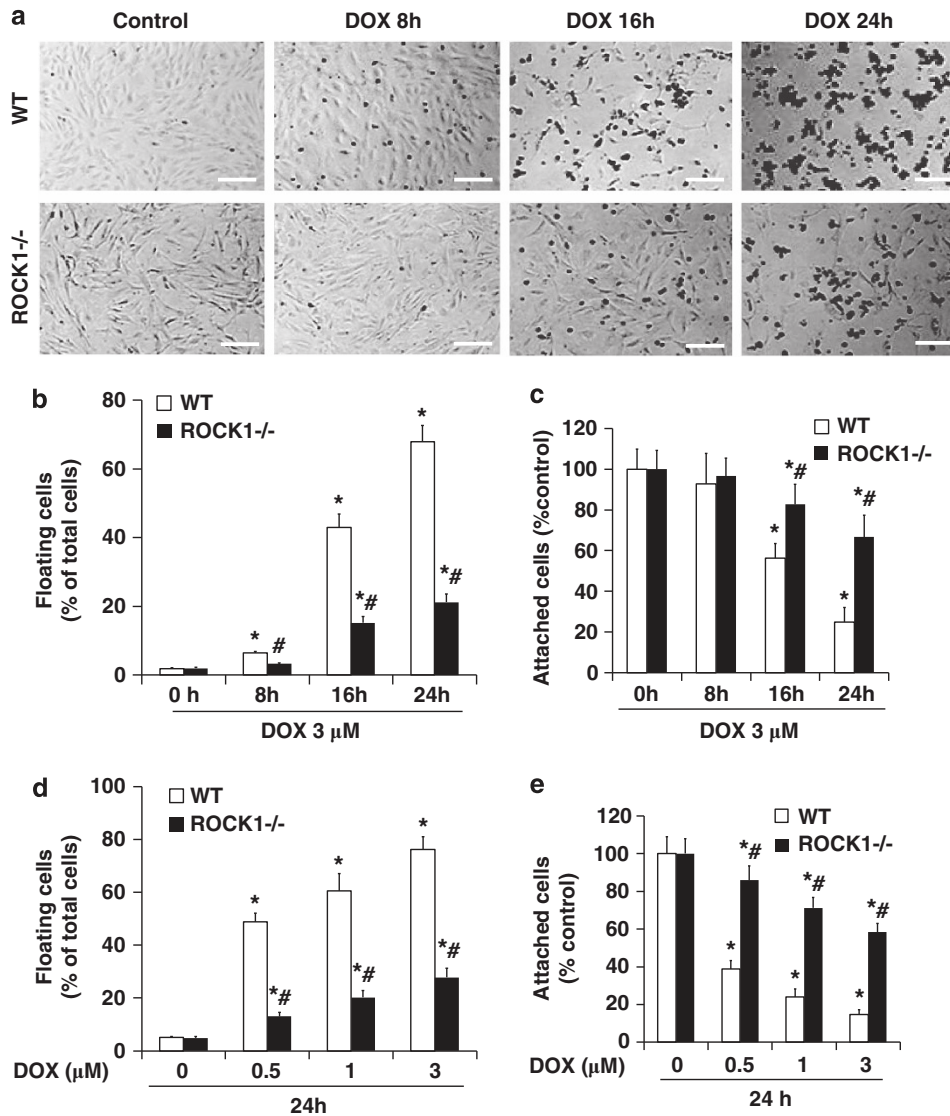


**Figure 2** ROCK1 deletion reduces cell detachment induced by doxorubicin. (a) Representative image of bright field photography of WT and *ROCK1*<sup>-/-</sup> cells treated with 3 μM doxorubicin at indicated time points showing doxorubicin-induced cell detachment. Bar, 400 μm. (b–e) Floating and attached cells were separately collected at indicated time points and dosages of doxorubicin. Floating cell ratio was expressed as percentage of total cells (floating plus attached cells) under indicated condition. Attached cell number was expressed as percentage of attached cells at baseline. \**P* < 0.05 versus control of the same genotype. \*\**P* < 0.05 versus WT under the same treatment condition

are located in the peripheral portion of the cell ('cortical actin'), and stress fibers, which are located in the central portion of the cell ('central stress fibers'). It has been shown that cells committed to detachment often exhibit disruption of central stress fibers and form a contractile ring at the cell periphery.<sup>29</sup> Phalloidin and phosphorylated MLC2 staining revealed that doxorubicin significantly increased the number of cells containing a cortical contractile ring and decreased the number of cells containing central stress fibers in WT cells (Figures 3a and b). In contrast, *ROCK1*<sup>-/-</sup> cells exhibited minimal cell shape alteration, a significantly less number of cells showing a cortical contractile ring and an increased number of cells with preserved central stress fibers compared with WT cells (Figures 3a and b).

**ROCK1 deficiency preferentially reduces MLC2 phosphorylation while preserving cofilin phosphorylation.** Phosphorylation of MLC2 has been shown to have essential roles in promoting actin disassembly and cell detachment in non-muscle cells.<sup>30,31</sup> Excessive myosin activity may destabilize central stress fibers.<sup>31,32</sup> We observed that doxorubicin treatment induced an increase in MLC2 phosphorylation, which could be detected within 30 min in WT MEFs (Figure 3c). In contrast, treatment had no significant effect on MLC2 phosphorylation in *ROCK1*<sup>-/-</sup> cells, which was reflected in a significantly lower level of phosphorylated MLC2 compared with WT cells (about 50% reduction, Figure 3c). These results indicate that ROCK1 deletion inhibits the increased actomyosin contraction induced by doxorubicin.

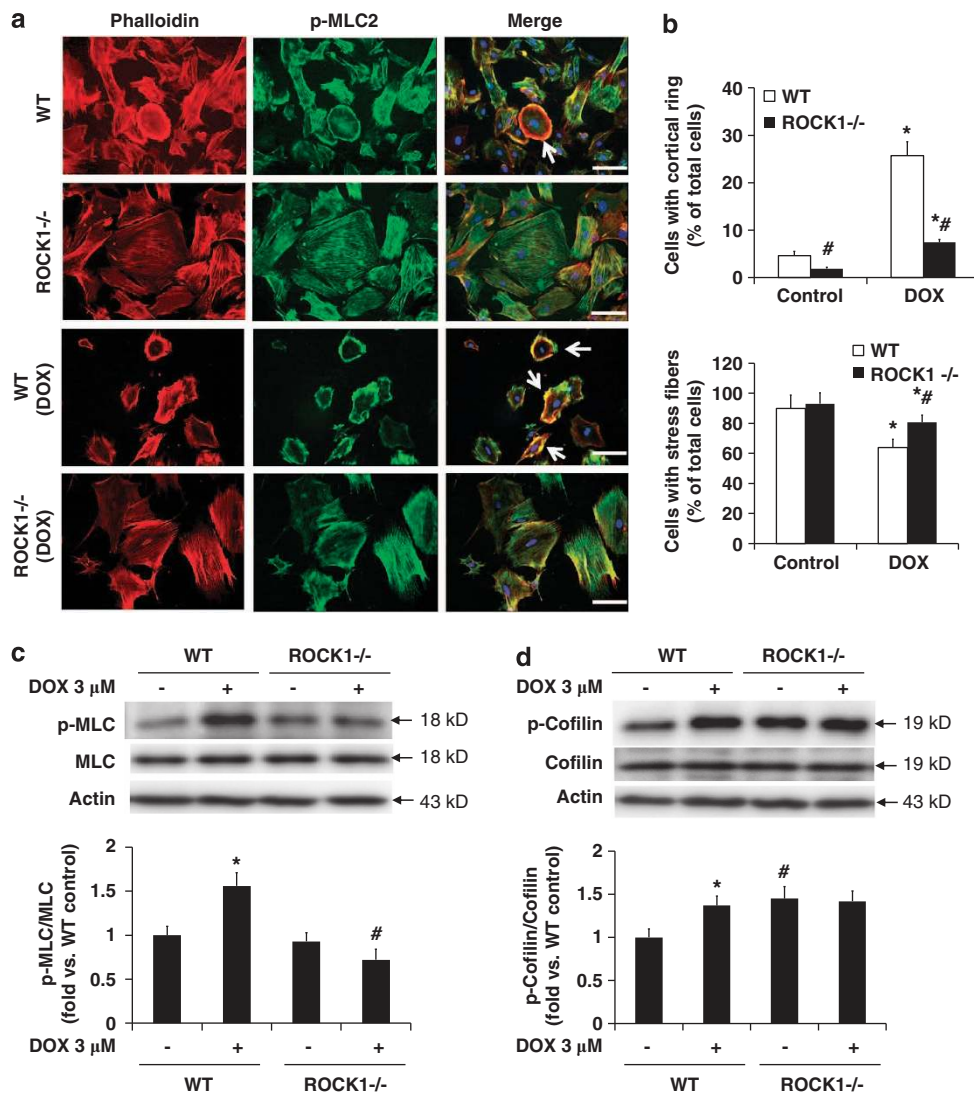


**Figure 3** ROCK1 deletion reduces actin cytoskeleton reorganization. (a) Representative images of rhodamine-phalloidin staining for F-actin (red), p-MLC staining (green), and DAPI staining (blue) of WT and *ROCK1*<sup>-/-</sup> cells treated with 3 μM doxorubicin for 16 h. Actomyosin contractile rings are indicated with white arrows. Bar, 100 μm. (b) Cells showing cortical contractile ring structure (top) or with nucleus crossed by stress fibers (bottom) were counted and expressed as percentage of total cells under indicated condition. For each treatment, over 1000 cells were counted. (c and d) Representative image (top) and quantitative analysis (bottom) of western blot of p-MLC2 and MLC2, or p-cofilin and cofilin in cell lysates from attached WT and *ROCK1*<sup>-/-</sup> MEFs treated with 3 μM doxorubicin for 30 min. Actin was used to confirm equal loading. \**P* < 0.05 versus control of the same genotype. #*P* < 0.05 versus WT under the same treatment condition



We also examined the phosphorylation status of cofilin, which reduces its actin depolymerization activity.<sup>7,8</sup> We noticed that doxorubicin treatment increased cofilin phosphorylation in WT cells, which was detectable within 30 min (Figure 3d). *ROCK1*<sup>-/-</sup> cells exhibited higher or similar levels of cofilin phosphorylation compared with WT cells at baseline or under doxorubicin treatment, respectively (Figure 3d). These results suggest that ROCK2 activation in ROCK1-deficient cells maintains the phosphorylation of cofilin, which was confirmed by the ROCK inhibitor study described below. Together, these results imply that doxorubicin treatment on one hand can induce MLC2 phosphorylation, which is dependent on ROCK1 to promote actomyosin contraction and cell detachment, and on the other hand, it can increase cofilin phosphorylation which is not dependent on ROCK1 (but likely on ROCK2) to maintain actin cytoskeleton stability and cell adhesion. The increased actomyosin contraction seems to have a predominant role leading to cell detachment.

**ROCK2 deficiency reduces both MLC2 and cofilin phosphorylation, but does not prevent cell detachment induced by doxorubicin.** Phalloidin stained *ROCK2*<sup>-/-</sup> cells exhibited significant reduction in the number of cells exhibiting a cortical contractile ring compared with WT cells (Figures 4a and b), a characteristic shared with *ROCK1*<sup>-/-</sup> cells. However, instead of increasing cortical ring formation, doxorubicin treatment increased periphery membrane folding in *ROCK2*<sup>-/-</sup> cells (Figures 4a and b), leading to an altered cell adhesion in *ROCK2*<sup>-/-</sup> cells. This morphological feature was not observed in *ROCK1*<sup>-/-</sup> cells at baseline or after doxorubicin treatment. Consistent with the increased periphery membrane folding, ROCK2 deletion does not prevent cell detachment induced by doxorubicin as *ROCK2*<sup>-/-</sup> cells exhibited a trend of an increased ratio of floating cells compared with that in WT cells (Figure 4c). Moreover, both MLC2 and cofilin phosphorylation were reduced by 20 or 50% in *ROCK2*<sup>-/-</sup> cells at baseline or

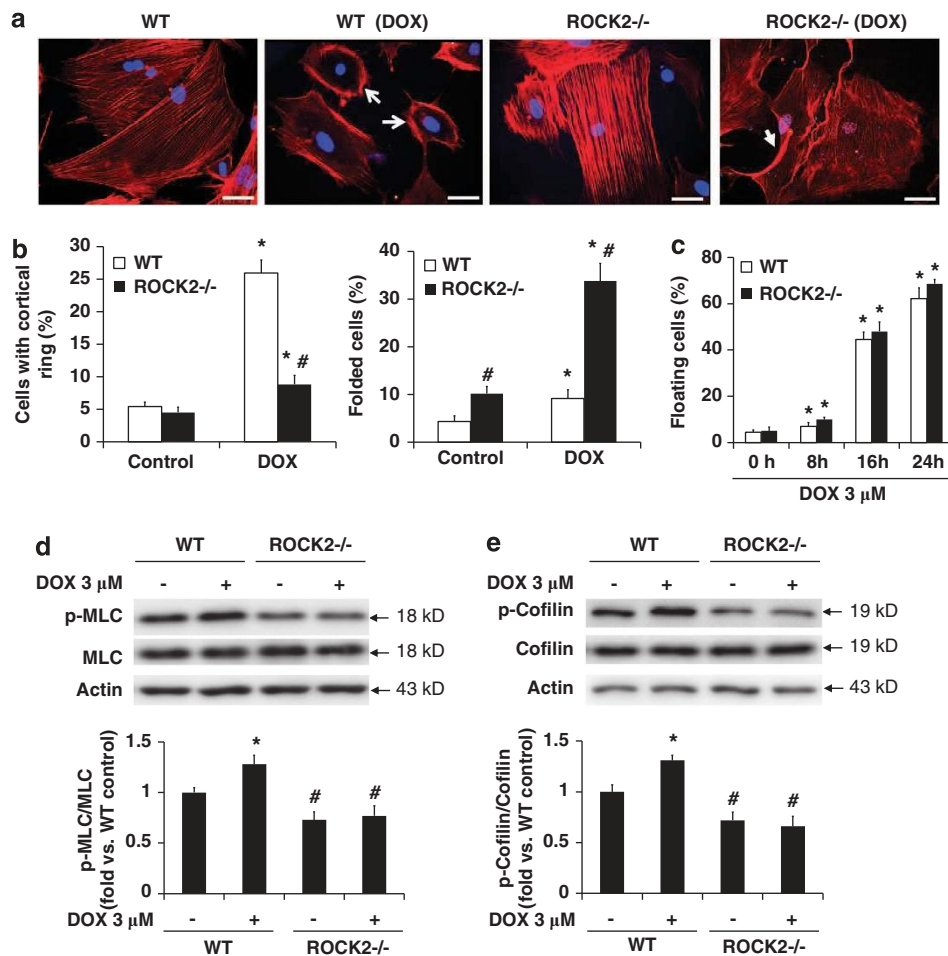


**Figure 4** ROCK2 deletion does not inhibit doxorubicin-induced cell detachment. (a) Representative images of rhodamine-phalloidin staining for F-actin (red) and DAPI staining (blue) of WT and *ROCK2*<sup>-/-</sup> cells treated with 3 μM doxorubicin for 16h. Actomyosin contractile rings are indicated with white arrow, and folded periphery membranes with white arrowheads. Bar, 50 μm. (b) Cells showing formation of cortical contractile ring structure or with folded periphery membrane were counted and expressed as percentage of total cells under indicated conditions. For each treatment, over 500 cells were counted. (c) Floating cells and attached cells were separately collected and counted at indicated time points and dosages of doxorubicin. Floating cell ratio was expressed as percentage of total cells (floating plus attached cells) under indicated conditions. (d and e) Representative image (top) and quantitative analysis (bottom) of western blot of p-MLC2 and MLC2, or p-cofilin and cofilin in cell lysates from attached WT and *ROCK2*<sup>-/-</sup> MEFs treated with 3 μM doxorubicin for 30 min. \**P* < 0.05 versus control of the same genotype. #*P* < 0.05 versus WT under the same treatment condition

after doxorubicin treatment, respectively (Figures 4d and e), indicating that ROCK2 deletion has a negative impact on actin cytoskeleton stability via inhibiting both MLC2 and cofilin phosphorylation.

**Inhibition of ROCKs by inhibitors promotes cell detachment induced by doxorubicin.** The inhibition of ROCKs by Y27632 resulted in the disruption of actin stress fibers in WT and *ROCK1*<sup>-/-</sup> cells (Figure 5a), consistent with the reported actions of ROCK pan-inhibitors.<sup>17</sup> This disruptive effect on stress fibers significantly increased doxorubicin-induced cell detachment in WT and *ROCK1*<sup>-/-</sup> cells (Figures 5b and c). As expected, Y27632 treatment significantly reduced the phosphorylation of MLC (20–50% reduction, Figure 5d) and cofilin (about 60–80% reduction, Figure 5e) at both baseline and doxorubicin treatment conditions in WT cells. Moreover, Y27632 treatment suppressed cofilin phosphorylation in *ROCK1*<sup>-/-</sup> cells to the same extent as in WT cells (Figure 6b). While MLC phosphorylation was reduced to a similar extent in *ROCK1*<sup>-/-</sup>, *ROCK2*<sup>-/-</sup>, or Y27632-treated MEFs, the

profile of cofilin phosphorylation was clearly different in these cells.

Small interfering ribonucleic acids (siRNA) specifically targeting ROCK1 or ROCK2 was also used to evaluate their contribution to the regulation of cytoskeleton stability. Endogenous ROCK1 or ROCK2 expression was reduced by 80–90% after transfection of their respective siRNA (Supplementary Figure 3A). ROCK1 siRNA-transfected cells, similar to *ROCK1*<sup>-/-</sup> cells, exhibited reduced cortical ring formation and preserved central stress fibers compared with the scrambled siRNA-transfected cells after doxorubicin treatment (Supplementary Figure 3B). ROCK2 siRNA-transfected cells showed increased periphery membrane folding, which was more prominent than that observed in *ROCK2*<sup>-/-</sup> cells at baseline condition. Double siRNA transfection resulted in the disruption of central stress fibers as observed in Y27632-treated cells.

**Caspase-independent mechanism is involved in doxorubicin-induced cell detachment.** The subsequent experiments were designed to address the mechanisms

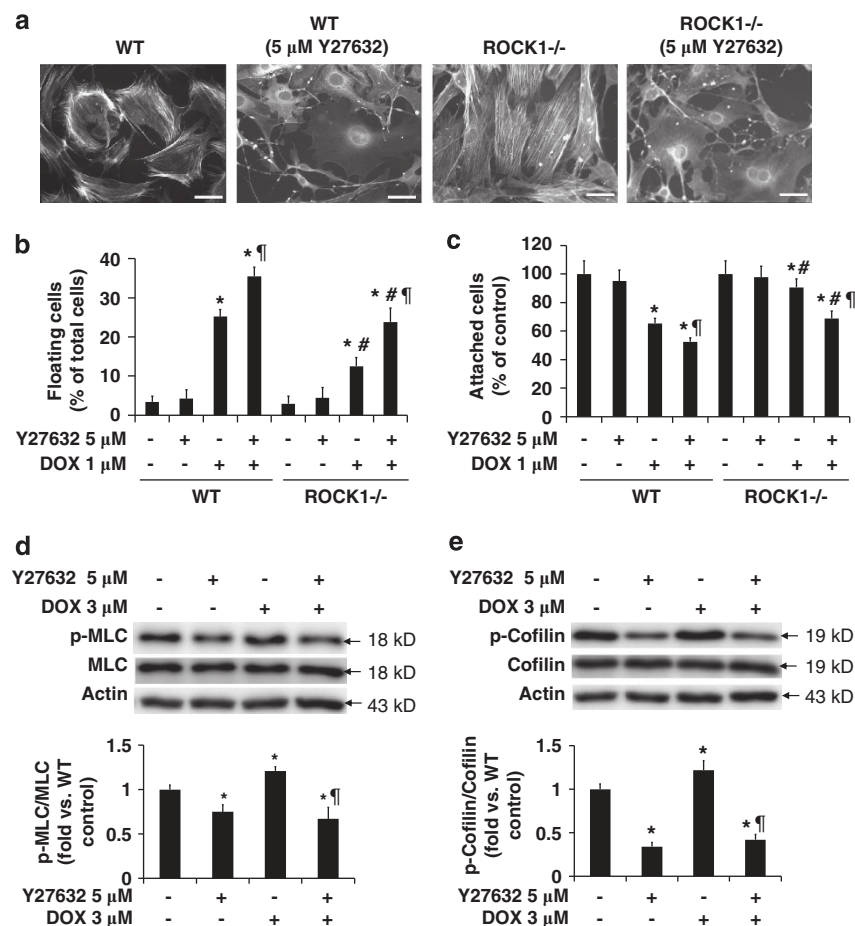


**Figure 5** Disruption of stress fibers by ROCK pan-inhibitor facilitates doxorubicin-induced detachment and death of attached cells. (a) Representative images of rhodamine-phalloidin staining for F-actin of WT and *ROCK1*-deficient cells treated with 5 μM Y27632 for 4 h. Bar, 50 μm. (b and c) Floating cells and attached cells were collected and counted after treatment with 1 μM doxorubicin and/or 5 μM Y27632 for 16 h. (d and e) Representative image (top) and quantitative analysis (bottom) of western blot of p-MLC2 and MLC2, or p-cofilin and cofilin in cell lysates from attached WT MEFs treated with 3 μM doxorubicin and/or 5 μM Y27632 for 30 min. The ratio of p-MLC to MLC or p-cofilin to cofilin was expressed as fold change relative to WT control. \**P* < 0.05 versus control of the same genotype. #*P* < 0.05 versus WT under the same treatment condition. ¶*P* < 0.05 versus WT under doxorubicin only condition

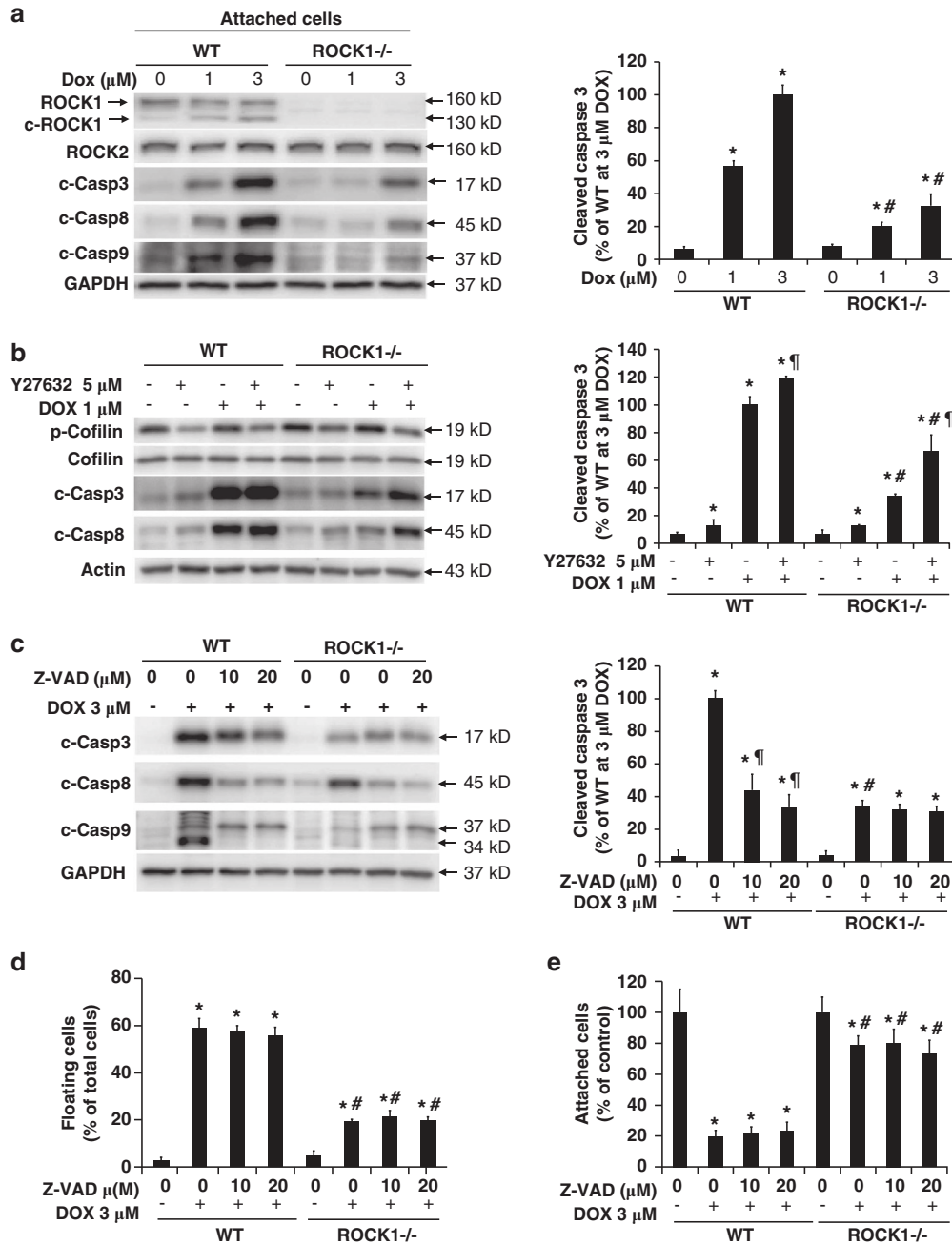


**Figure 6** Treatment with pan-caspase inhibitor does not reduce cell detachment induced by doxorubicin. (a) Representative image (left panel) of western blot of full length and cleaved ROCK1 and cleaved caspase-3, -8, and -9 in cell lysates from attached WT and *ROCK1*<sup>-/-</sup> MEFs treated for 16 h with increasing dosages of doxorubicin as indicated. Quantitative analysis (right panel) of immunoreactive bands of cleaved capsase-3 ( $n = 4-6$  for each condition), expressed as percent change relative to WT cells treated with doxorubicin. (b) Representative image (left) and quantitative analysis (for cleaved capsase-3, right) of western blot of p-cofilin, cofilin, cleaved caspase-3, and -8 in cell lysates from attached WT MEFs treated for 16 h with 1 μM doxorubicin and/or 5 μM Y27632. (c) Representative image (left panel) and quantitative analysis (for cleaved capsase-3, right) of western blot of cleaved caspase-3, -8, and -9 in cell lysates from total WT and *ROCK1*<sup>-/-</sup> MEF cells collected after 16 h treatment with 3 μM doxorubicin and various concentrations of z-VAD-fmk, a pan-caspase inhibitor, showing inhibition of caspase activation by caspase inhibitor. (d and e) Floating cells and attached cells were collected. Floating cell ratio was expressed as percentage of total cells (floating plus attached cells) under indicated conditions. Attached cell number was expressed as percentage of attached cells at baseline. \* $P < 0.05$  versus control of the same genotype. \*\* $P < 0.05$  versus WT under the same treatment condition. † $P < 0.05$  versus the same genotype under doxorubicin only condition

involved in ROCK1-mediated cell detachment induced by doxorubicin. It is known that caspase activation is involved in cell detachment,<sup>29</sup> to some extent mediated by

caspase-3-mediated ROCK1 activation to promote cell detachment through increasing MLC2 phosphorylation.<sup>33,34</sup> Consistent with the established pro-apoptotic action of

doxorubicin,<sup>23,24</sup> doxorubicin treatment elicited a dose-dependent increase of cleaved caspase-3, -8, and -9 (indicators of an increase in apoptosis) and cleaved ROCK1 in WT cells (Figure 6a). Interestingly the level of caspase activation was significantly reduced in *ROCK1*<sup>-/-</sup> cells (Figure 6a). Consistent with the reduced caspase activation, annexin V positivity was decreased in *ROCK1*<sup>-/-</sup> cells (Figure 7d, Supplementary Figure 4A). In addition, ROCK inhibitor treatment augmented caspase activation in WT and *ROCK1*<sup>-/-</sup> cells (Figure 6b). These results support a correlation between caspase activation and cell detachment. However, the cotreatment with 10 and 20  $\mu\text{M}$  z-VAD-fmk, a pan-caspase inhibitor, had no inhibitory effect on cell detachment in WT and *ROCK1*<sup>-/-</sup> cells (Figures 6d and e), even though the caspase activation was obviously lowered (Figure 6c), signifying that doxorubicin-induced cell detachment occurs independently of caspase activation.

### ROCK1 deficiency does not inhibit apoptosis in detached cells.

Cell detachment from extracellular matrix is also a potent apoptotic inducer.<sup>35</sup> Agreeing with this concept, we observed that the expression levels of cleaved caspase-3, -8, and -9 in WT cells were at least 20-fold higher in the floating cells compared with the attached cells after 16 h treatment (Figure 7a). Annexin V staining also demonstrated marked differences between floating and attached cells (Figure 7d). In contrast to the attached cells, the levels of cleaved caspase-3, -8, and -9 in the floating cells were independent of the dosages and durations of doxorubicin treatment (Figures 7b and c), indicating that after detachment, apoptosis occurs independently of doxorubicin. In addition, ROCK1 deficiency did not reduce the levels of cleaved caspase-3, -8, and -9 and annexin V positivity in floating cells (Figures 7c and d, Supplementary Figure 4B) showing that ROCK1 deficiency has no significant inhibitory effect on apoptosis occurring after detachment.

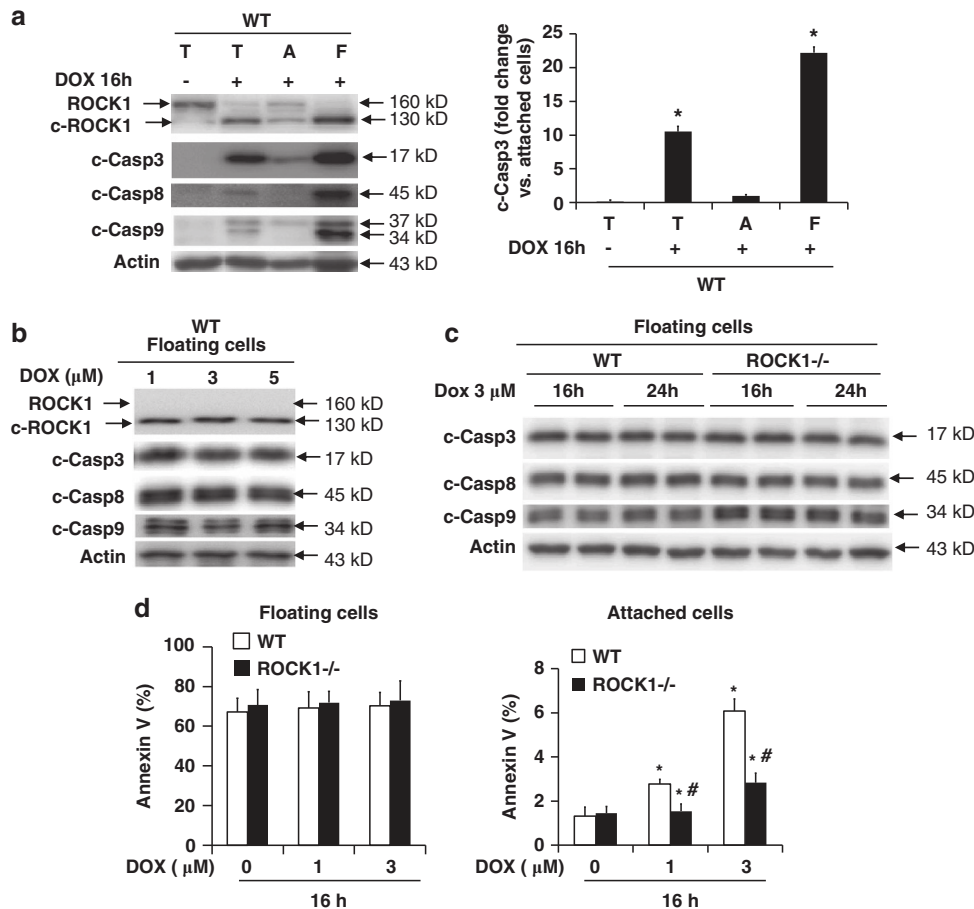


**Figure 7** ROCK1 deletion does not inhibit apoptosis in detached cells. (a) Representative image (left panel) of western blot of ROCK1, cleaved caspase-3, -8, and -9 in cell lysates from total (T), attached (A) and floating (F) WT cells treated for 16 h with 3  $\mu\text{M}$  doxorubicin. Densitometry analysis (right panel) of immunoreactive bands of cleaved caspase-3. Expression of cleaved caspase-3 was expressed as fold change relative to attached cells after doxorubicin treatment. \* $P < 0.05$  versus doxorubicin-treated attached cells. (b) Representative image of western blot of cleaved caspase-3, -8, and -9 in cell lysates from floating WT cells collected after 16 h of treatment with increasing dosages of doxorubicin as indicated. (c) Representative image of western blot of cleaved caspase-3, -8, and -9 in cell lysates from floating WT and *ROCK1*<sup>-/-</sup> MEFs collected after 16 h or 24 h treatment with 3  $\mu\text{M}$  doxorubicin. (d) Apoptotic cell ratio was determined by annexin V staining followed by FACS analysis in floating (left) and attached (right) cells collected after treatment for 16 h with increasing dosages of doxorubicin as indicated. \* $P < 0.05$  versus control of the same genotype. # $P < 0.05$  versus WT under the same treatment condition



**Inhibition of actomyosin contraction and disruption of stress fiber formation produce opposite effects on doxorubicin-induced detachment and apoptosis.**

We subsequently validated the contribution of increased actomyosin contraction and stress fiber instability to doxorubicin-induced cell detachment and apoptosis using pharmacologic inhibitors, blebbistatin, and cytochalasin D. Blebbistatin is a direct inhibitor of myosin II ATPase activity,<sup>36</sup> and cytochalasin D inhibits actin polymerization.<sup>37</sup> Blebbistatin treatment (1 or 2  $\mu$ M) partially mimics the inhibitory effects of ROCK1 deletion on doxorubicin-induced cell detachment and apoptosis (Figure 8). Blebbistatin decreased the number of cells with a cortical contractile ring (Figures 8a and b), reduced cell detachment (the ratio of

floating cells was about 40% for cotreatment *versus* 60% for doxorubicin alone) (Figures 8c and d), improved cell viability (Figure 8e), and attenuated caspase activation (Figure 8f) of the WT cells compared with doxorubicin treatment alone. In addition, blebbistatin had no significant effect on *ROCK1*<sup>-/-</sup> cells. Together, our data support the notion that the beneficial effects of ROCK1 deletion are partially attributable to the reduced actomyosin contraction via inhibition of MLC2 phosphorylation.

Treatment with 0.2  $\mu$ M cytochalasin D disrupted stress fibers, and increased cell detachment similarly in WT and *ROCK1*<sup>-/-</sup> cells (Supplementary Figure 5). Cotreating with doxorubicin further exaggerated doxorubicin-induced cell detachment and caspase activation in attached cells. These

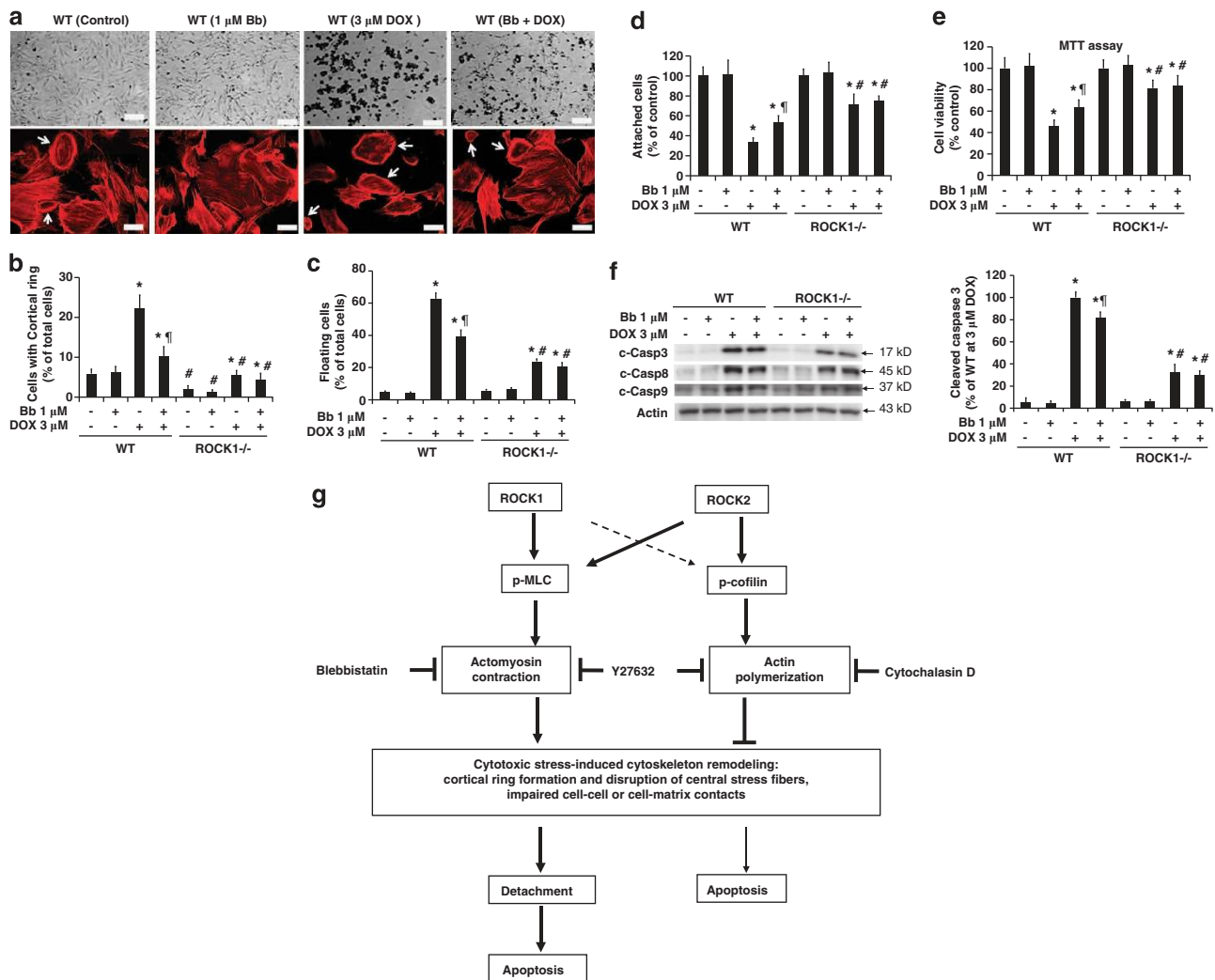


**Figure 8** Inhibition of actomyosin contraction by blebbistatin partially mimics effects of ROCK1 deletion. (a) Representative images of bright field photography (top) and rhodamine-phalloidin staining for F-actin (bottom) of WT and *ROCK1*<sup>-/-</sup> cells treated with 3  $\mu$ M doxorubicin and/or 1  $\mu$ M blebbistatin for 16 h. Actomyosin contractile rings are indicated with white arrows. Bar, 400  $\mu$ m (top), 100  $\mu$ m (bottom). The same treatment condition was used for the following panels (b–f). (b) Cells showing formation of cortical contractile ring structure were counted. (c and d) Floating cells and attached cells were collected and counted. (e) MTT assay was performed. (f) Representative image (left panel) of western blot of cleaved caspase-3, -9, and -8 in cell lysates from attached WT and *ROCK1*-deficient MEF cells. Densitometry analysis (right panel) of immunoreactive bands of cleaved caspase-3 expressed as percent change relative to WT cells treated with 3  $\mu$ M doxorubicin. \**P* < 0.05 *versus* control of the same genotype. #*P* < 0.05 *versus* WT under the same treatment condition. †*P* < 0.05 *versus* the same genotype under doxorubicin only condition. (g) Schematic summary of roles of ROCK1 and ROCK2 in regulating actin cytoskeleton reorganization induced by cytotoxic stress (e.g., doxorubicin), leading to cell detachment and apoptosis. The thick lines stand for dominating actions. The thin lines stand for minor actions. The broken lines stand for alternative actions in the absence of dominating actions

detrimental effects of cytochalasin D on WT and ROCK1-deficient cells are similar to those produced by ROCK inhibitors in response to doxorubicin treatment. Together, these data further support the notion that the beneficial effects of ROCK1 deletion are in part mediated through preservation of actin cytoskeleton stability.

## Discussion

The present study reveals the distinct roles of ROCK isoforms in regulating actin cytoskeleton reorganization and cell detachment induced by doxorubicin. By utilizing a combined genetic and pharmacological approach, our results support the concept that ROCK1 is involved in destabilizing actin cytoskeleton through regulating MLC2 phosphorylation and peripheral actomyosin contraction, whereas ROCK2 is required for stabilizing actin cytoskeleton through regulating cofilin phosphorylation. Their distinct actions on actin cytoskeleton remodeling contribute to their different effects on cell detachment.

Previous studies using ROCK inhibitors and/or ROCK dominant active/negative mutants support that ROCK activity is required for stress fiber organization and cell adhesion through promoting both myosin activity and actin polymerization.<sup>5–8,38</sup> Our studies, with isoform-selective deletions of ROCK, dissociate ROCK-dependent peripheral (ROCK1 and ROCK2 dependent) and central stress fiber organization (mainly ROCK2 dependent). This dissociation is likely due to separating ROCK-dependent MLC2 phosphorylation (ROCK1 and ROCK2 dependent) from ROCK-dependent cofilin phosphorylation (mainly ROCK2 dependent). However, in the absence of ROCK2, ROCK1 is involved in regulating cofilin phosphorylation and central stress fiber organization as the reduction of cofilin phosphorylation and disruption of central stress fibers were less severe in ROCK2-deficient cells than in ROCK inhibitor-treated cells. Together, our results reveal a preferential role of endogenous ROCK2 in regulating cofilin phosphorylation, and also suggest an alternative role for ROCK1 when ROCK2 activity is absent. The mechanisms underlying the differential effects of ROCK1 and ROCK2 on cofilin phosphorylation remain to be determined. The specificity could be related with the differences in their coil-coiled domains (55% sequence identity) and PH domains (66% sequence identity),<sup>1–4</sup> which may contribute to their different activation profiles by RhoA, different lipid-binding preferences of the PH domains, and different subcellular localizations.<sup>39</sup> Although our results suggest that cofilin phosphorylation is involved in the differential effects of ROCK1 and ROCK2 on central stress fiber disassembly, ROCK has additional substrates that may also contribute to the distinct actions of ROCK isoforms. Future studies are needed to dissect the mechanisms underlying the isoform specificity for cofilin phosphorylation, and possibly for other ROCK targets.

Our results also reveal that ROCK1 deletion attenuates caspase activation in attached cells upon doxorubicin treatment. This inhibitory effect is mediated, at least in part, by reduced actomyosin contraction as supported by the observations that blebbistatin treatment partially mimics antiapoptotic effects of ROCK1 deletion. The preservation of central actin stress fibers also contributes to the reduced caspase

activation, as supported by the fact that the treatment with cytochalasin D could boost caspase activation. Apoptosis can be induced by a loss of survival signals due to impairment or loss of cell–cell or cell–matrix interactions, a process termed anoikis.<sup>35</sup> Actin cytoskeleton reorganization leading to the formation of cortical rings and the disappearance of central stress fibers represents an early step of anoikis.<sup>29</sup> This mechanism likely contributes to the doxorubicin-induced apoptosis as the cytoskeleton features of anoikis were observed in WT cells. These results suggest that ROCK1 deletion inhibits actin cytoskeleton reorganization induced by doxorubicin treatment, and consequently preserves cell–matrix interaction and inhibits caspase activation. It is somewhat unexpected that the treatment with caspase inhibitor did not prevent cell detachment induced by doxorubicin. Previous studies suggest that caspase-3-mediated ROCK1 activation promotes cell detachment through increasing MLC phosphorylation.<sup>29,33,34,40</sup> In the current study, we detected an increase in MLC phosphorylation within 30 min after starting doxorubicin treatment, which is before detectable caspase activation. Our results suggest that doxorubicin induces cell detachment through ROCK1-dependent but not caspase-dependent activation of myosin.

Our findings with ROCK1-deficient MEFs share some similarity with pro-survival effects of ROCK inhibitors in preventing anoikis in some contexts including embryonic stem cells grown in suspension culture conditions.<sup>41–43</sup> In addition, our data from using ROCK inhibitors share some similarity with pro-apoptotic effects of ROCK inhibitors in other cell contexts.<sup>44–46</sup> Depending on the cell type and the apoptotic stimulus, ROCK activity, can act either as a pro-apoptotic or as a pro-survival regulator. The pro-apoptotic effects of ROCK inhibitors were mainly observed in the adhesion-dependent and differentiated cells. The current study demonstrates that when placed MEF cells under the same stress conditions ROCK1 deletion can exert pro-survival effects, whereas ROCK inhibitors produce pro-apoptotic effects. It is worth noting that the antiapoptotic property of ROCK1 deletion observed in this study is consistent with our previous *in vivo* observations that ROCK1 deletion inhibits cardiomyocyte apoptosis in cardiac decompensation,<sup>47,48</sup> and also in hematopoietic stem cells under stressed erythropoiesis.<sup>49</sup> Together, these studies support the notion that ROCK1 may represent an attractive therapeutic target to limit tissue damages due to increased apoptosis under certain pathological conditions.<sup>21,47,48</sup> It will be of interest to determine if the pro-survival characteristics of ROCK1 deficiency observed in normal cells in response to doxorubicin could be extended to tumor cells, which would then promote chemoresistance. Our recent study indicates that in contrast to normal cells, ROCK1 deletion reduces survival of oncogene-bearing cells, which exhibit different cytoskeletal organizations compared with normal cells.<sup>50</sup> Future studies are needed to evaluate the roles of ROCK1 and ROCK 2 in cancer cells with aberrant expression and/or activity of ROCK in response to chemotherapeutic agents.

Recent studies with siRNA-based gene silencing have shown that ROCK1 and ROCK2 have functional differences in regulating actin cytoskeleton in a variety of cell types.<sup>39,51–58</sup> These studies have mainly addressed stress fiber assembly

and cell adhesion, but did not focus on the effects of isoform knockdown on cell detachment and death. In agreement with previous studies characterizing *ROCK1*<sup>-/-</sup> or *ROCK2*<sup>-/-</sup> MEFs,<sup>52</sup> we observed that the architecture of actin cytoskeleton in *ROCK1*<sup>-/-</sup> or *ROCK2*<sup>-/-</sup> MEF cells was largely similar compared with the WT MEFs at baseline condition, although we detected a slight reduction in the number of cells with cortical ring formation in *ROCK1*<sup>-/-</sup> MEFs (1.89% versus 4.62% in WT cells) and a slight increase in the number of cells with periphery membrane folding in *ROCK2*<sup>-/-</sup> MEFs (10.2% versus 4.32% in WT cells). These subtle differences between WT cells and ROCK1 or ROCK2-deficient cells were amplified under stress conditions.

In summary, this study has shown that ROCK1 deletion, ROCK2 deletion, and pan-ROCK inhibitors produce different effects on actin stress fiber disassembly, leading to the different consequences on cell de-adhesion under stressed condition. A model to summarize all of these findings is schemed in Figure 8g. During the last decade, ROCK family has attracted significant interest as a promising target for the treatment of a wide range of human diseases, including cardiovascular disorders, neurologic disorders, metabolic disorders, and cancers.<sup>9–16</sup> The current observations should be valuable for further understanding the beneficial and detrimental effects of ROCK pan-inhibitors in experimental and clinical studies, and also for supporting the development of isoform-selective ROCK1 inhibitors.

## Materials and Methods

**Cell culture and treatments.** MEF cells of global ROCK1-deficient mice in FVB background<sup>22</sup> were prepared from E13.5 embryos using standard procedures. Briefly, E13.5 embryos were obtained from FVB WT and *ROCK1* knockout mice. Genomic DNA was extracted from brain tissues for genotyping. The embryonic tissues were minced in phosphate-buffered saline (PBS) containing trypsin after removing liver and intestine tissues, followed by pipetting to further dissociate cells from tissues. The MEF cells were collected by centrifugation, then resuspended and plated in Dulbecco's modified Eagle's medium (DMEM; Life Technologies, Grand Island, NY, USA) supplemented with 10% fetal bovine serum (FBS; Atlanta Biologicals, Lawrenceville, GA, USA) and penicillin–streptomycin in a humidified incubator with 5% CO<sub>2</sub> at 37 °C. Cells at 90% confluency were treated with various drugs at indicated times and dosages. These drugs include pan-ROCK inhibitor Y27632, pan-caspase inhibitor z-VAD-fmk, and blebbistatin from Enzo Life Sciences (Farmingdale, NY, USA); doxorubicin and cytochalasin D from Sigma (Beverly, MA, USA).

Targeted deletion of a genomic fragment containing exon 2 of *ROCK2* gene was accomplished by homologous recombination in C57BL/6 genetic background (Supplementary Figure 1). Deletion of exon 2 results in a frame-shift mutation in ROCK2, removing all residues from the residue 47 to the end of the protein. Successful targeting and deletion of *ROCK2* were confirmed by Southern blotting, PCR, and western blot (Figure 1a, and Supplementary Figure 1). Heterozygous *ROCK2* mice in C57BL/6 background were backcrossed to FVB background for more than eight generations. Homozygous deletion of *ROCK2* on FVB background is embryonically lethal. ROCK2-deficient MEF cells were prepared as described above from E13.5 *ROCK2* homozygous knockout embryos derived from interbreeding of *ROCK2* heterozygous mice in FVB background. All animal experiments were conducted in accordance with the National Institutes of Health 'Guide for the Care and Use of Laboratory Animals' (NIH Publication No. 85–23, revised 1996) and were approved by the Institutional Animal Care and Use Committee at Indiana University School of Medicine.

**Fluorescence imaging.** To detect F-actin, MEF cells were seeded and attached to gelatin-coated glass coverslips. The cells were fixed with 4% paraformaldehyde in PBS for 15 min and permeabilized with 0.2% Triton X-100 for 30 min. After blocking with 5% bovine serum albumin, the cells were stained with rhodamine-conjugated phalloidin (Life Technologies). For visualization of p-MLC2,

after blocking with 5% goat serum in PBS for 60 min, the cells were incubated with rabbit polyclonal antibodies to p-MLC2(Ser19) (#3671; Cell Signaling, Beverly, MA, USA) overnight followed by incubation with Alexa Fluor 488-conjugated goat anti-rabbit IgG (Life Technologies). The glass coverslips were mounted in Vectashield mounting media (Vector Laboratories, Burlingame, CA, USA) containing diamidino-2-phenylindole (DAPI) to counterstain the nuclei. The fluorescent images were taken with Leica DM5500B microscope (objectives: HCX PL FUOTAR 20.0 × 0.50, HCX PL FUOTAR 40 × 0.75; Bannockburn, IL, USA) equipped with a DFC300FXR2 camera, and analyzed with the Leica AF6000 software (Bannockburn, IL, USA).

**Protein analysis.** Following treatment with desired drugs, cells were washed with cold PBS, solubilized with Tris lysis buffer (20 mM Tris, pH 7.5, 1% Triton X-100, 100 mM NaCl, 5 mM EDTA plus proteinase, and phosphatase inhibitors (Roche, Indianapolis, IN, USA)) or with LAS buffer (50 mM PIPES, pH6.9, 50 mM NaCl, 5 mM MgCl<sub>2</sub>, 5 mM EGTA, 5% glycerol, 0.1% Nonidet P-40, 0.1% Triton X-100, 0.1% Tween 20, 0.1% 2-mercaptoethanol, 0.001% Antifoam C plus protease inhibitor cocktail) for 30 min with shaking at 4 °C. Cell lysates were then cleared by centrifugation at 15 000 × g at 4 °C for 15 min, the supernatant was then resolved on 8% or 10% SDS-PAGE gels, transferred to polyvinylidene difluoride membrane (Bio-Rad, Hercules, CA, USA). The blots were then probed with primary antibodies to ROCK1 (#sc-5560; Santa Cruz Biotechnology, Santa Cruz, CA, USA), ROCK2 (#sc-5561), caspase 8 (#sc-7890), MYPT1 (#07-672; Millipore, Billerica, MA, USA), p-MYPT1(Thr696) (#ABS45), caspase-3 (#9662; Cell Signaling), cleaved caspase-3 (#9661), caspase 9 (#9504), cleaved caspase 9 (#9509), cleaved caspase 8 (#9429), PARP (#9542), cofilin (#3312), p-cofilin(Ser3) (#3311), MLC2 (#3672), p-MLC2(Ser19) (#3671), LIMK1 (#3842), and p-LIMK1(Thr508)/LIMK2(Thr505) (#3841). After washing with buffer, the membranes were blotted with corresponding secondary antibodies conjugated with horseradish peroxidase. The membranes were developed with ECL western blotting or SuperSignal West Pico Chemiluminescent Substrate (Thermo Scientific, Hanover Park, IL, USA), and the blots were visualized by using the Fujifilm LAS-4000 Imager (Piscataway, NJ, USA). All blots were normalized to GAPDH (#AM4300; Ambion, Austin, TX, USA) or to actin (#sc-1616; Santa Cruz).

**Cell viability and detachment assays.** Following treatment with desired drugs, cell viability was determined by measuring the activity of enzymes that reduce MTT by the colorimetric assay.<sup>59</sup> In a 24-well plate, 1 × 10<sup>5</sup> cells/well were seeded with 1 ml of culture media and exposed to various drugs for indicated time periods. The media was removed and replaced with 1 ml of DMEM with 0.5 mg of MTT (without phenol red and FBS) for 4 h. After removing the MTT-containing DMEM, the remaining formazan blue crystals were dissolved in 1 ml of DMSO. Absorbance at 540 nm was measured using a microplate reader (iMark microplate reader; Bio-Rad). The percentage of cell survival was calculated as the A<sub>540</sub> value of treated cells divided by the A<sub>540</sub> of control cells in wells of the same culture dish without treatment multiplied by 100. The samples were prepared in triplicates, and the absorption value is the average of three measurements. At least three independent experiments were analyzed.

Following treatment with desired drugs, detached cells in culture medium (floating cells) were collected at indicated times and counted with a hemacytometer. The attached cells were harvested by trypsinization and resuspended in culture medium for counting. Cell viability of floating and attached cells was also determined by assessing cellular uptake of trypan blue dye (#T8154; Sigma). Briefly, cell suspension was mixed with equal volume of 0.4% trypan blue solution and counted for trypan blue positive and negative within 2 min. At least three independent experiments were analyzed for each condition.

**Flow cytometry.** Following treatment with desired drugs, the attached or floating MEF cells were collected. Apoptosis and dead cells were determined by live staining of the cells with annexin V-FITC (Apoptosis Detection Kit; BD Biosciences, San Jose, CA, USA) and 7-amino-actinomycin D (7-AAD), respectively. Briefly, harvested cells were incubated in binding buffer 30 min at room temperature, followed by incubation with annexin V-FITC and 7-AAD as outlined in the manufacturer's instructions. All samples were analyzed using Becton Dickinson FACSCalibur and CellQuest software (San Jose, CA, USA). The samples were prepared in triplicate, and each cell preparation was analyzed twice.

**Transfection of siRNA.** siRNA was introduced into MEF cells by transient transfection with X-tremeGENE siRNA Transfection Reagent (Roche). MEF cells



were transfected at 60% confluency. The SMARTpool siRNAs for murine ROCK1 and ROCK2 were purchased from Dharmacon, Thermo Scientific (Pittsburgh, PA, USA). siRNAs, prediluted in 100  $\mu$ l of Opti-MEM I (Gibco; Life Technologies), was combined with X-tremeGENE siRNA transfection reagent diluted in 100  $\mu$ l of Opti-MEM I medium as recommended by the manufacturer. The mixture was incubated for 20 min at room temperature for complex formation and added drop-wisely to cells. The final siRNA concentration was 80 nM. At 72 h post-transfection, cells were treated as indicated and followed by western blot analysis or fluorescence imaging.

**Statistical analysis.** Data are reported as mean  $\pm$  S.E. Comparisons between groups were analyzed by Student's *t*-test or ANOVA as appropriate, with  $P < 0.05$  considered as significant.

### Conflict of Interest

The authors declare no conflict of interest.

**Acknowledgements.** This work was supported by National Institutes of Health grants (HL085098 to LW), a Grant-in-Aid award from American Heart Association, Midwest Affiliate (to LW) and the Riley Children's Foundation.

### Author contributions

JS designed and performed experiments, analyzed data and wrote the manuscript; XW played a key role in performing experiments. MS, LZ and YY performed experiments. SV and RK contributed with reagents and to manuscript preparation. LW designed experiments, analyzed data and wrote the manuscript.

- Matsui T, Amano M, Yamamoto T, Chihara K, Nakafuku M, Ito M *et al*. Rho-associated kinase, a novel serine/threonine kinase, as a putative target for small gtp binding protein rho. *EMBO J* 1996; **15**: 2208–2216.
- Ishizaki T, Maekawa M, Fujisawa K, Okawa K, Iwamatsu A, Fujita A *et al*. The small gtp-binding protein rho binds to and activates a 160 kda ser/thr protein kinase homologous to myotonic dystrophy kinase. *EMBO J* 1996; **15**: 1885–1893.
- Nakagawa O, Fujisawa K, Ishizaki T, Saito Y, Nakao K, Narumiya S. Rock-i and rock-ii, two isoforms of rho-associated coiled-coil forming protein serine/threonine kinase in mice. *FEBS Lett* 1996; **392**: 189–193.
- Leung T, Chen XQ, Manser E, Lim L. The p160 rhoa-binding kinase rok alpha is a member of a kinase family and is involved in the reorganization of the cytoskeleton. *Mol Cell Biol* 1996; **16**: 5313–5327.
- Amano M, Ito M, Kimura K, Fukata Y, Chihara K, Nakano T *et al*. Phosphorylation and activation of myosin by rho-associated kinase (rho-kinase). *J Biol Chem* 1996; **271**: 20246–20249.
- Kimura K, Ito M, Amano M, Chihara K, Fukata Y, Nakafuku M *et al*. Regulation of myosin phosphatase by rho and rho-associated kinase (rho-kinase). *Science* 1996; **273**: 245–248.
- Maekawa M, Ishizaki T, Boku S, Watanabe N, Fujita A, Iwamatsu A *et al*. Signaling from rho to the actin cytoskeleton through protein kinases rock and lim-kinase. *Science* 1999; **285**: 895–898.
- Ohashi K, Nagata K, Maekawa M, Ishizaki T, Narumiya S, Mizuno K. Rho-associated kinase rock activates lim-kinase 1 by phosphorylation at threonine 508 within the activation loop. *J Biol Chem* 2000; **275**: 3577–3582.
- Hahmann C, Schroeter T. Rho-kinase inhibitors as therapeutics: From pan inhibition to isoform selectivity. *Cell Mol Life Sci* 2010; **67**: 171–177.
- Loirand G, Pacaud P. The role of rho protein signaling in hypertension. *Nat Rev Cardiol* 2010; **7**: 637–647.
- Miyamoto S, Del Re DP, Xiang SY, Zhao X, Florholmen G, Brown JH. Revisited and revised: Is rhoa always a villain in cardiac pathophysiology? *J Cardiovasc Transl Res* 2010; **3**: 330–343.
- Nunes KP, Rigby CS, Webb RC. Rhoa/rho-kinase and vascular diseases: what is the link? *Cell Mol Life Sci* 2010; **67**: 3823–3836.
- Dong M, Yan BP, Liao JK, Lam YY, Yip GW, Yu CM. Rho-kinase inhibition: a novel therapeutic target for the treatment of cardiovascular diseases. *Drug Discov Today* 2010; **15**: 622–629.
- Amano M, Nakayama M, Kaibuchi K. Rho-kinase/rock: A key regulator of the cytoskeleton and cell polarity. *Cytoskeleton (Hoboken)* 2010; **67**: 545–554.
- Surma M, Wei L, Shi J. Rho kinase as a therapeutic target in cardiovascular disease. *Future Cardiol* 2011; **7**: 657–671.
- Olson MF. Applications for rock kinase inhibition. *Curr Opin Cell Biol* 2008; **20**: 242–248.
- Uehata M, Ishizaki T, Satoh H, Ono T, Kawahara T, Morishita T *et al*. Calcium sensitization of smooth muscle mediated by a rho-associated protein kinase in hypertension. *Nature* 1997; **389**: 990–994.
- Asano T, Ikegaki I, Satoh S, Suzuki Y, Shibuya M, Takayasu M *et al*. Mechanism of action of a novel antivasospasm drug, ha1077. *J Pharmacol Exp Ther* 1987; **241**: 1033–1040.
- Davies SP, Reddy H, Caivano M, Cohen P. Specificity and mechanism of action of some commonly used protein kinase inhibitors. *Biochem J* 2000; **351**: 95–105.
- Bain J, Plater L, Elliott M, Shpiro N, Hastie CJ, McLauchlan H *et al*. The selectivity of protein kinase inhibitors: a further update. *Biochem J* 2007; **408**: 297–315.
- Shi J, Zhang L, Wei L. Rho-kinase in development and heart failure: insights from genetic models. *Pediatr Cardiol* 2011; **32**: 297–304.
- Zhang YM, Bo J, Taffet GE, Chang J, Shi J, Reddy AK *et al*. Targeted deletion of rock1 protects the heart against pressure overload by inhibiting reactive fibrosis. *Faseb J* 2006; **20**: 916–925.
- Di Marco A, Gaetani M, Scarpinato B. Adriamycin (nsc-123,127): a new antibiotic with antitumor activity. *Cancer Chemother Rep* 1969; **53**: 33–37.
- Shi J, Zhang L, Zhang YW, Surma M, Payne RM, Wei L. Down-regulation of doxorubicin-induced myocardial apoptosis accompanies postnatal heart maturation. *Am J Physiol Heart Circ Physiol* 2012; **302**: H1603–H1613.
- Zhang YW, Shi J, Li YJ, Wei L. Cardiomyocyte death in doxorubicin-induced cardiotoxicity. *Arch Immunol Ther Exp (Warsz)* 2009; **57**: 435–445.
- Sawyer DB, Peng X, Chen B, Pentassuglia L, Lim CC. Mechanisms of anthracycline cardiac injury: can we identify strategies for cardioprotection? *Prog Cardiovasc Dis* 2010; **53**: 105–113.
- Feng Z, Chen B, Tang SC, Liao K, Chen WN, Chan V. Effect of cytoskeleton inhibitors on deadhesion kinetics of hepg2 cells on biomimetic surface. *Colloids Surf B Biointerfaces* 2010; **75**: 67–74.
- Colombo R, Dalle Donne I, Milzani A. Metal ions modulate the effect of doxorubicin on actin assembly. *Cancer Biochem Biophys* 1990; **11**: 217–226.
- Mills JC, Stone NL, Pittman RN. Extracellular apoptosis. The role of the cytoplasm in the execution phase. *J Cell Biol* 1999; **146**: 703–708.
- Vicente-Manzanares M, Ma X, Adelstein RS, Horwitz AR. Non-muscle myosin ii takes centre stage in cell adhesion and migration. *Nat Rev Mol Cell Biol* 2009; **10**: 778–790.
- Szczepanowska J, Korn ED, Brzeska H. Activation of myosin in hela cells causes redistribution of focal adhesions and f-actin from cell center to cell periphery. *Cell Motil Cytoskeleton* 2006; **63**: 356–374.
- Zagorska A, Deak M, Campbell DG, Banerjee S, Hirano M, Aizawa S *et al*. New roles for the lkb1-nuak pathway in controlling myosin phosphatase complexes and cell adhesion. *Sci Signaling* 2010; **3**: ra25.
- Sebbagh M, Renvoize C, Hamelin J, Riche N, Bertoglio J, Breard J. Caspase-3-mediated cleavage of rock i induces mlc phosphorylation and apoptotic membrane blebbing. *Nat Cell Biol* 2001; **3**: 346–352.
- Coleman ML, Sahai EA, Yeo M, Bosch M, Dewar A, Olson MF. Membrane blebbing during apoptosis results from caspase-mediated activation of Rock I. *Nat Cell Biol* 2001; **3**: 339–345.
- Frisch SM, Screamor RA. Anokiis mechanisms. *Curr Opin Cell Biol* 2001; **13**: 555–562.
- Kovacs M, Toth J, Hetenyi C, Malnasi-Csizmadia A, Sellers JR. Mechanism of blebbistatin inhibition of myosin ii. *J Biol Chem* 2004; **279**: 35557–35563.
- May JA, Ratan H, Glenn JR, Losche W, Spangenberg P, Heptinstall S. Gpiib-iiiia antagonists cause rapid disaggregation of platelets pre-treated with cytochalasin d. Evidence that the stability of platelet aggregates depends on normal cytoskeletal assembly. *Platelets* 1998; **9**: 227–232.
- Kato K, Kano Y, Noda Y. Rho-associated kinase-dependent contraction of stress fibres and the organization of focal adhesions. *J R Soc Interface* 2011; **8**: 305–311.
- Yoneda A, Multhaupt HA, Couchman JR. The rho kinases i and ii regulate different aspects of myosin ii activity. *J Cell Biol* 2005; **170**: 443–453.
- Wang X, Lin G, Martins-Taylor K, Zeng H, Xu RH. Inhibition of caspase-mediated anoikis is critical for basic fibroblast growth factor-sustained culture of human pluripotent stem cells. *J Biol Chem* 2009; **284**: 34054–34064.
- Watanabe K, Ueno M, Kamiya D, Nishiyama A, Matsumura M, Wataya T *et al*. A rock inhibitor permits survival of dissociated human embryonic stem cells. *Nat Biotechnol* 2007; **25**: 681–686.
- Koyanagi M, Takahashi J, Arakawa Y, Doi D, Fukuda H, Hayashi H *et al*. Inhibition of the rho/rock pathway reduces apoptosis during transplantation of embryonic stem cell-derived neural precursors. *J Neurosci Res* 2008; **86**: 270–280.
- Braam SR, Nauw R, Ward-van Oostwaard D, Mummery C, Passier R. Inhibition of rock improves survival of human embryonic stem cell-derived cardiomyocytes after dissociation. *Ann N Y Acad Sci* 2010; **1188**: 52–57.
- Svoboda KK, Moessner P, Field T, Acevedo J. Rock inhibitor (y27632) increases apoptosis and disrupts the actin cortical mat in embryonic avian corneal epithelium. *Dev Dyn* 2004; **229**: 579–590.
- Moore M, Marroquin BA, Gugliotta W, Tse R, White SR. Rho kinase inhibition initiates apoptosis in human airway epithelial cells. *Am J Respir Cell Mol Biol* 2004; **30**: 379–387.
- Shi J, Wei L. Rho kinase in the regulation of cell death and survival. *Arch Immunol Ther Exp (Warsz)* 2007; **55**: 61–75.
- Chang J, Xie M, Shah VR, Schneider MD, Entman ML, Wei L *et al*. Activation of rho-associated coiled-coil protein kinase 1 (rock-1) by caspase-3 cleavage plays an



- essential role in cardiac myocyte apoptosis. *Proc Natl Acad Sci USA* 2006; **103**: 14495–14500.
48. Shi J, Zhang YW, Yang Y, Zhang L, Wei L. Rock1 plays an essential role in the transition from cardiac hypertrophy to failure in mice. *J Mol Cell Cardiol* 2010; **49**: 819–828.
49. Vemula S, Shi J, Mali RS, Ma P, Liu Y, Hanneman P *et al*. Rock1 functions as a critical regulator of stress erythropoiesis and survival by regulating p53. *Blood* 2012; **120**: 2868–2878.
50. Mali RS, Ramdas B, Ma P, Shi J, Munugalavadla V, Sims E *et al*. Rho kinase regulates the survival and transformation of cells bearing oncogenic forms of kit, flt3, and bcr-abl. *Cancer Cell* 2011; **20**: 357–369.
51. Yoneda A, Ushakov D, Mulhaupt HA, Couchman JR. Fibronectin matrix assembly requires distinct contributions from rho kinases i and -ii. *Mol Biol Cell* 2007; **18**: 66–75.
52. Noguchi M, Hosoda K, Fujikura J, Fujimoto M, Iwakura H, Tomita T *et al*. Genetic and pharmacological inhibition of rho-associated kinase ii enhances adipogenesis. *J Biol Chem* 2007; **282**: 29574–29583.
53. Wang Y, Zheng XR, Riddick N, Bryden M, Baur W, Zhang X *et al*. Rock isoform regulation of myosin phosphatase and contractility in vascular smooth muscle cells. *Circ Res* 2009; **104**: 531–540.
54. Mong PY, Wang Q. Activation of rho kinase isoforms in lung endothelial cells during inflammation. *J Immunol* 2009; **182**: 2385–2394.
55. Bryan BA, Dennstedt E, Mitchell DC, Walshe TE, Noma K, Loureiro R *et al*. Rho/rock signaling is essential for multiple aspects of vegf-mediated angiogenesis. *Faseb J* 2010; **24**: 3186–3195.
56. Lock FE, Hotchin NA. Distinct roles for rock1 and rock2 in the regulation of keratinocyte differentiation. *PLoS One* 2009; **4**: e8190.
57. Chun KH, Araki K, Jee Y, Lee DH, Oh BC, Huang H *et al*. Regulation of glucose transport by rock1 differs from that of rock2 and is controlled by actin polymerization. *Endocrinology* 2012; **153**: 1649–1662.
58. Darenfed H, Dayanandan B, Zhang T, Hsieh SH, Fournier AE, Mandato CA. Molecular characterization of the effects of  $\gamma$ -27632. *Cell Motil Cytoskeleton* 2007; **64**: 97–109.
59. Mosmann T. Rapid colorimetric assay for cellular growth and survival: application to proliferation and cytotoxicity assays. *J Immunol Methods* 1983; **65**: 55–63.



**Cell Death and Disease** is an open-access journal published by Nature Publishing Group. This work is licensed under the Creative Commons Attribution-NonCommercial-No Derivative Works 3.0 Unported License. To view a copy of this license, visit <http://creativecommons.org/licenses/by-nc-nd/3.0/>

Supplementary Information accompanies the paper on Cell Death and Disease website (<http://www.nature.com/cddis>)